A DFT and HF quantum chemical study of the tin nanocluster $[(RSn)_{12}O_{14}(OH)_6]^{2+}$ and its interactions with anions and neutral nucleophiles: confrontation with experimental data

Ricardo Vivas-Reyes,[ab] Frank De Proft,[b] Paul Geerlings,*[b] Monique Biesemans,[c] Rudolph Willem,[c] François Ribot[d] and Clément Sanchez[d]

[a] *Grupo de Quimica Cuantica y Teorica, Chemistry Department, Cartagena University, A.A 1661, Cartagena, Colombia*
[b] *Eenheid Algemene Chemie (ALGC), Free University of Brussels (VUB), Pleinlaan 2, B-1050, Brussel, Belgium. E-mail: pgeerlin@vub.ac.be; Fax: +33.2.629.3317; Tel: +33.2.629.3314*
[c] *High Resolution NMR Center (HNMR), Free University of Brussels (VUB), Pleinlaan 2, B-1050, Brussel, Belgium*
[d] *Laboratoire de Chimie de la Matière Condensée (CNRS UMR 7574), Tour 54, 5e étage Université Pierre et Marie Curie, 4 Place Jussieu, F-75252, Paris cedex 05, France*

Received (in Montpellier, France) 5th February 2002, Accepted 2nd April 2002
First published as an Advance Article on the web 30th July 2002

Calculations of traditional wave function and DFT based reactivity descriptors are reported for the nanocluster $[(RSn)_{12}O_{14}(OH)_6]^{2+}$ (R = CH_3) in order to get insight into the factors determining the exact nature of its interactions with anions or neutral nucleophiles (F^-, Cl^-, OH^-, H_2O, acetone, DMSO). Two levels of calculation (Hartree–Fock and DFT) were used in this study, giving the opportunity to compare the performance of both aproaches. As a whole the HF and DFT results, despite some numerical differences, are qualitatively and in most cases quantitatively similar, since no interchanges in the sequences are found. Calculated charge distributions indicate that the hexacoordinated tin atoms are expected to be harder, the pentacoordinated ones softer. This result is confirmed by the condensed local softness and experimental observations provided by the literature (X-ray, ^{119}Sn NMR), thereby matching predictions made on the basis of the HSAB principle. Molecular electrostatic potential (MEP) calculations further confirm this selectivity, indicating that nucleophiles will approach preferentially the macrocation around the poles rather than at the equator of the cage. Calculated stabilization energies indicate that the charged (F^-, Cl^- and OH^-) and uncharged (DMSO, acetone and water) nucleophiles tested all interact preferentially with the cage pole region around the hexacoordinated tin atoms. This feature appears related to the electrostatic nature of the interaction for the charged nucleophiles and to the tendency, for all the nucleophiles, to form hydrogen bridges with the μ_2-OH moieties. The basicity of the three types of oxygen atoms [μ_2-OH, μ_3-O(I), μ_3-O(P)] present in $[(RSn)_{12}O_{14}(OH)_6]^{2+}$ has been addressed by protonation energy and MEP calculations, taking into account accessibility factors not represented by atomic charges. Summarizing, it turns out that the hardness/softness properties of tin atoms are modulated by their coordination; however, the sole consideration of these quantities is not sufficient to predict in all cases the strength and orientation of the interaction between various nucleophiles and the cluster, since electrostatic interactions and H-bonding play a major role.

A large number of monoorganotin oxo-clusters with complexing ligands (carboxylates, phosphinates, dialkylphosphates) bound to the metallic centers have been described and reviewed in the second half of the eighties.[1] Since then, new monoorganotin oxo-clusters, which do not contain any complexing ligands, have been described.[2–4] Among the latter type, the dicationic cluster of general formula $[(RSn)_{12}O_{14}(OH)_6]^{2+}$ (Fig. 1), has received particular and extensive interest during the last decade.[3,5–15] Several synthetic approaches have been proposed[3,5,6,8–10] and it has been recognized as a versatile nanobuilding block for the design of hybrid organic-inorganic materials.[11–16]

The first $[(RSn)_{12}O_{14}(OH)_6]^{2+}$ cation based compounds have been isolated in the crystalline state as dichlorides $[(RSn)_{12}O_{14}(OH)_6]Cl_2$, with R = *i*-Pr[3] and *n*-Bu.[5] As a result of the search for alternatives to hydrolysis-based syntheses[3,5,6,8] and the interest in the influence of the nature of the counteranions on the structure and the behavior of such compounds, the $[(nBuSn)_{12}O_{14}(OH)_6]^{2+}$ cation has likewise been isolated as the dihydroxide,[6] and the diacetate,[14] the bis(diphenylphosphinate)[7] and the bis(*p*-toluenesulphonate)salts.[9,10] When available, single crystal X-ray diffraction data[3,5,6,10] reveals a very constant molecular structure for the nanodication, in contrast with the remarkable versatility and complexity of the long range order induced by counteranions, solvent molecules and hydrogen bonding. The molecular structure of the $[(RSn)_{12}(\mu_3\text{-}O)_{14}(\mu_2\text{-}OH)_6]^{2+}$ dication is a centrosymmetric cage with twelve tin atoms linked by μ_3-O bridges (Fig. 1).[3,5,6,10] The six tin atoms located at the "cage equator" are five-coordinate and have a distorted square pyramidal geometry. The three tin atoms of each of the two "cage poles" are six-coordinate and have a distorted octahedral geometry involving also μ_2-OH bridges. Such a molecular framework has also been described, with only minor variations, for $[(^i PrOTi)_{12}(\mu_3\text{-}O)_{14}(\mu_2\text{-}O)_2(\mu_2\text{-}O^i Pr)_4]$,[17] $[(OV)_{12}(\mu_3\text{-}O)_{12}(\mu_3\text{-}F)_2(\mu_2\text{-}OH)_6]^{6-}$ [18] and $[(^i PrSn)_{11}(OV)(\mu_3\text{-}O)_{14}(\mu_2\text{-}OH)_6]^+$.[19]

 DOI: 10.1039/b201328b

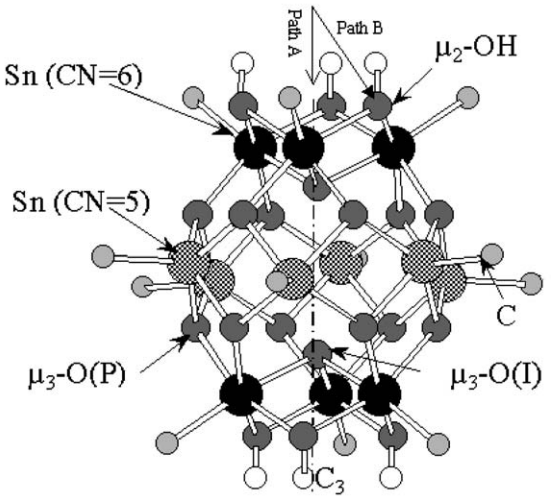

Fig. 1 Schematic structure of the macrocation $[(RSn)_{12}O_{14}(OH)_6]^{2+}$. Only the carbon (C) of the R groups directly bound to tin are shown for clarity; CN = coordination number. The two paths (A and B) considered for a nucleophile X approaching the polar region of the cage are also indicated.

In the crystalline state, the two monovalent counteranions, needed to balance the positive charge of $[(RSn)_{12}O_{14}(OH)_6]^{2+}$, are centro-symmetrically located at the "cage poles". They are involved in a complex network of hydrogen bonds including the μ_2-OH bridges and, in most cases, small molecules with oxygen [H_2O, DMF, ^{i}PrOH, DMPU = 1,3-dimethyl-2,4,5,6-tetrahydro-2(1*H*)-pyrimidinone].[3,5,6,10] The cage structures reported in the solid state exhibit symmetry considerably lower than the symmetry evidenced in solution by ^{119}Sn NMR.[5–7,9,10,14] When considering the averaged cylindrical symmetry of the organic R group on the NMR time scale in solution, the cage has basically a D_{3d} symmetry, as supported by the only two ^{119}Sn resonances (around −280 and −450 ppm for the butyltin derivatives), which are associated with the five- and six-coordinate tin atoms, respectively. The C_3 axis passes through the two μ_3-O atoms bridging the three six-coordinate tin atoms at each "cage pole" and the σ planes are defined by the C_3 axis and a pair of centrosymmetric five-coordinate tin atoms at the "cage equator". The three C_2 axes, perpendicular to the C_3 axis, naturally arise from the inversion center and the σ planes, to which they are perpendicular. One can note that this spectroscopically averaged D_{3d} symmetry is observed in solution even when the anions have a lower symmetry (*i.e.*, $CH_3CO_2^-$,[14] $Ph_2PO_2^-$,[7] p-$CH_3C_6H_4SO_3^-$[10]).

Several experimental investigations have evidenced interactions between this tin oxo-cluster and anions or neutral nucleophiles.[3,5–7,9,10,14] However, a thorough understanding of the factors determining the exact nature of these interactions has yet to be reached. There is little doubt that the anions interact basically with the cage poles,[3,5–7,9,10,14] but whether this interaction is purely electrostatic, or involves μ_2-OH mediated hydrogen bonding or is an orbital determined Lewis acid-base interaction, remains a matter of discussion. Also, the factors that determine whether ionic dissociation prevails or not in solution, the extent of the latter having been shown to be both anion and solvent dependent,[7,9,10] have not been clearly established. Finally, some NMR data indicate that small nucleophilic molecules (dioxane, THF, DMSO, pyridine) can interact with the five-coordinate equatorial tin atoms,[7,10,20] but other data also indicate that the "cage poles" can be affected by the addition of neutral nucleophiles.[9,10] The possible determinants of this variability, such as basicity, nucleophilicity, polarizability, and/or softness of the donor, have not been clearly identified so far.

All these issues prompted us to wonder whether these questions could be answered or, at least, clarified by a non-empirical theoretical approach. First, one can hope that theoretical descriptors could provide indications, or at least trends, as to what factors affect the structural properties of the $[(RSn)_{12}O_{14}(OH)_6]^{2+}$ cation and its interactions with nucleophiles, whether anionic or neutral. More particularly, such an approach is expected to shed some light onto the role of hydrogen bonding, and, as far as the cage poles are concerned, to offer a clear discrimination between tin-coordination based and purely electrostatic interactions. Second, *ab initio* approaches to reactivity descriptors in organotin chemistry are, to the best of our knowledge, unexplored in the literature. Existing non-empirical theoretical studies on tin derivatives essentially concentrated on structure and stability,[21–25] with, recently, transition state calculations for homolytic substitution reactions on stannane and methylstannane,[26] or compared calculated geometries with those from X-ray diffraction analysis in order to assess the influence of packing effects on structures.[27] Very recently two papers appeared in the literature that deal with tin(IV) compounds using the HF method in combination with the LanL2DZ pseudopotential approach, investigating the electronic structure of dimethyl tin(IV) moieties in interaction with a DNA model system and dimethyl and trimethyl tin(IV) complexes of porphyrin derivatives. This level of calculations was justified in view of the time consuming aspects of these studies.[28] The present authors presented a study on group properties (electronegativity, hardness) to explain the evolution of the ^{119}Sn chemical shift in tetracoordinated Sn compounds of the type $CH_3SnRR'R''$, where R, R′ and R″ are organic groups or halogens.[29]

In this context, applying DFT methods[30] on the systems considered is interesting in its own and the comparison of DFT and HF for these large, tin containing compounds, deserves a thorough assessment. Moreover, the use of DFT based descriptors of reactivity[30] is unprecedented in Sn containing compounds.

A variety of reactivity descriptors, such as the molecular charge distribution and the atomic electronic populations, derived from it, can be found in the literature.[31] The molecular electrostatic potential (MEP)[32] has been found to be adequate for describing electrostatic (*i.e.*, non-orbital based) interactions, and has been used in recent years to study the structure and reactivity of polyoxometallate cages.[33] Besides these traditional reactivity descriptors, density functional theory[30] (DFT) based descriptors, such as the Fukui function and (local) hardness and softness,[34,35] have gained widespread use in recent years, by some of the present authors among others, for the study of softer (*i.e.*, orbital based) interactions in which Pearson's hard and soft acids and bases (HSAB) principle[36,37] acts as the guiding principle.[38–40] Moreover, if the HSAB principle is applied in a local sense,[41] regioselectivity problems can be addressed on the basis of the idea that soft (respectively hard) regions of one reaction partner will preferentially interact with soft (respectively hard) regions of the other partner.[42–46]

This paper deals with the calculation of such local quantities for the idealized macrocation $[(MeSn)_{12}O_{14}(OH)_6]^{2+}$ (Fig. 1) with two goals. First, the scope and limitations of such computational methods for macrocations containing the tin atom, so far unexplored in the more general context of heavier elements included in cage structures, are assessed. Second, we aim at comparing the results of our calculations with various experimental observations, mainly based on NMR and X-ray diffraction, about the interactions of the macrocation $[(RSn)_{12}O_{14}(OH)_6]^{2+}$ with nucleophiles.[3,5–7,9,10,14,20] As these interactions do not seem straightforward to rationalize on an intuitive basis, it is hoped that a theoretical approach based on reactivity descriptors could shed some light onto the donor-acceptor interaction properties of such nanoclusters. The conditions for such a comparison between calculations

and experiments appear ideal in the present case because of the broad panel of experimental data available.

Theory

As a detailed presentation and discussion of reactivity parameters can be found elsewhere,[30,40] only the relevant expressions used for the evaluation of different quantities for the macrocation $[(RSn)_{12}O_{14}(OH)_6]^{2+}$ are given here.

The global hardness (η) and the global softness (S) are calculated from eqns. (1) and (2):

$$\eta = (\varepsilon_{LUMO} - \varepsilon_{HOMO})/2 \quad (1)$$

$$S = 1/(2\eta) \quad (2)$$

where ε_{LUMO} is the energy of the lowest unoccupied orbital and ε_{HOMO} is the energy of the highest occupied orbital.

For the calculation of the Fukui[30,34,47] function f^+ we used the condensed approach proposed by Yang and Mortier,[48] using the gross Mulliken[31] charge at atom A, q_A, for the systems with N and $N+1$ electrons, calculated at the same geometry:

$$f_A^+ = q_A(N+1) - q_A(N) \quad (3)$$

According to the relation $s(\underline{r}) = Sf(\underline{r})$, the corresponding condensed local softness parameters can easily be calculated from the condensed Fukui function and the global softness; for instance:

$$s_A^+ = Sf_A^+ \quad (4)$$

In order to investigate the interactions of the macrocation with different nucleophiles, electrostatic based indicators (atomic charges, MEP), together with DFT based quantities, such as local softness, were evaluated.

The MEP, $V(\underline{r})$, calculated in the usual way, neglecting polarization and nuclear rearrangement effects due to the presence of a unit test charge at the distance $\underline{r}$, is given by:

$$V(\underline{r}) = \sum_A \frac{Z_A}{|\underline{R}_A - \underline{r}|} - \int \frac{\rho(\underline{r}')}{|\underline{r}' - \underline{r}|} d\underline{r}' \quad (5)$$

where the summation runs over all nuclei A with charge Z_A and coordinate $\underline{R}_A$. $V(\underline{r})$ represents the potential exerted at coordinate $\underline{r}$ by the nuclei and the electrons.

Originally, the MEP was used to obtain information on the molecular regions that are preferred in an electrophilic attack.[32] Yet, as previously reported,[49–51] the preference for a nucleophilic attack can also be investigated with the MEP, as done in the present work.

Computational details

The atomic charges used in the condensed Fukui function evaluation were obtained with the Mulliken[31] population analysis. Potential driven CHELPG[52] charges were also tried but were not used in the Fukui function analysis because negative values were obtained systematically.

The MEP has been computed for two particular planes of the macrocation.. The first one, P1, [Fig. 2(a)] corresponds to a plane of symmetry (σ) that contains tin atoms of both coordinations. The second one, P2, [Fig. 2(b)] is perpendicular to the previous one and passes only through two tin atoms (a five- and a six-coordinate) that belong to the same four-membered cycle.

In this work, two levels of calculation were used. Originally the Hartree–Fock/LanL2DZ level was adopted using the Lan2DZ[53–55] pseudopotential approach for all atoms. Later on we turned to the DFT B3LYP[56] level with 6-31G*[57] basis sets for C, H and O and the LanL2DZ[53–55] pseudopotential basis set for tin. In these calculations the different interactions between the nanocluster and the nucleophiles were optimized partially. The stabilization energies were calculated with optimized geometries. However, because of the huge size of the systems, the optimizations were made as follows: (*i*) the internal geometries of the cage and of the nucleophiles were kept frozen and (*ii*) the nucleophiles were moved along one line defined by the nucleophiles (F^- and Cl^-) or its oxygen atom (OH^-, H_2O, acetone and DMSO) and one atom of the cage (*i.e.*, an oxygen of a μ_2-OH, an "internal" μ_3-O or a penta-coordinated tin atom). Under such conditions, the relative orientation of the nucleophiles involving more than one atom remains unchanged during the optimization process and the distance between one atom of the cage and of the atom of the nucleophile is the only optimized variable.

For these aspects the DFT level can be expected to be superior to the HF level.[58] Nevertheless, for the sake of comparison HF calculations were included as they are less time consuming, taking into consideration the size of a system containing 12 Sn atoms. Because of too demanding calculation time requirements, this work has been carried out on an ideal methyltin derivative with a perfect D_{3d} symmetry. The spatial coordinates of the D_{3d}-$[(MeSn)_{12}O_{14}(OH)_6]^{2+}$ macrocation were

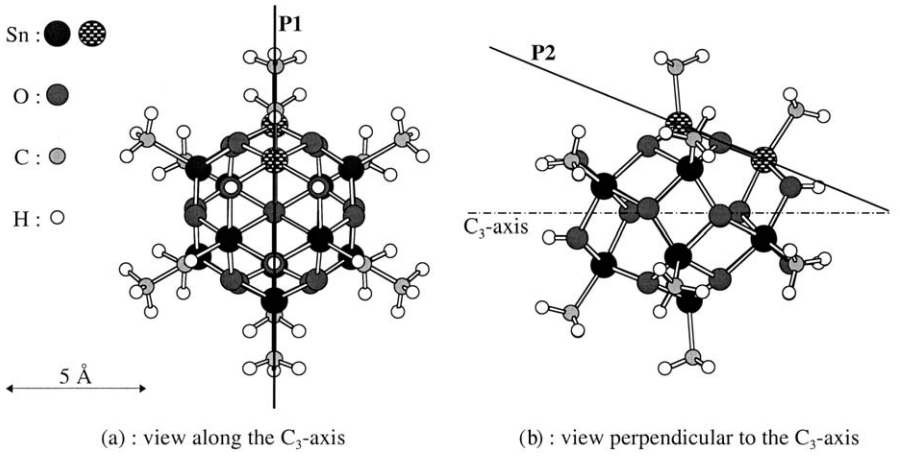

Fig. 2 (a) Projection of the macrocation on a plane perpendicular to the C_3 axis. The vertical black line represents the trace of the plane P1, which is normal to the projection plane and corresponds to a symmetry plane σ of the D_{3d} point group. The MEP contour plot of Fig. 3 has been calculated for the plane P1. (b) Projection of the macrocation on the plane P1. The tilted black line represents the trace of the plane P2, perpendicular to the plane P1 and containing one six-coordinate (right) and one five-coordinate (left) tin atom. The latter two tin atoms are hatched in (a) and (b). The MEP contour plot of Fig. 4 has been calculated for the plane P2.

computed in order to reproduce, within 1%, the averaged Sn–O, Sn–C and Sn···Sn distances and O–Sn–O, O–Sn–C and Sn–O–Sn angles obtained from the X-ray structure of $[(BuSn)_{12}O_{14}(OH)_6]^{2+}(4\text{-}CH_3C_6H_4SO_3\text{-})_2{\cdot}C_4H_8O_2$.[10] The protons of the μ_2-OH were placed at 1 Å from the corresponding oxygen atoms with the O–H bond parallel to the C_3 axis. The other hydrogen atoms were placed according to the overall D_{3d} symmetry and the classical geometry of methyl groups, d(C–H) = 1.08 Å and angle H–C–H = 109°.

In a final step, the stabilization energy of the macrocation $[(MeSn)_{12}O_{14}(OH)_6]^{2+}$ in the presence of various nucleophiles, either charged or uncharged and of variable softness (F^-, OH^-, Cl^-, H_2O, acetone and DMSO), was determined with the nucleophile in the neighborhood of the pentacoordinated (equator) or hexacoordinated (poles) tin atoms. The calculations at the HF level using the LanL2DZ basis were refined for the basis set superposition error (BSSE) using the counterpoise correction.[59]

In order to determine the basicity of each of the three kinds of oxygen atoms present in the molecule, an "acidic" proton was placed at a fixed distance of 1.0 Å from this oxygen and the energy of the corresponding conjugate acid was computed. This distance reflects the O–H distance of 1.011 Å in the H_3O^+ cation of *p*-toluene sulfonic acid monohydrate, as determined by neutron diffraction.[60] The three different types of oxygen atoms in the cage have been considered (Fig. 1): (*i*) the six μ_2-OH, each bridging two six-coordinate tin atoms at the cage pole, (*ii*) the two "internal" μ_3-O(I), each bridging the three six-coordinate tin atoms of a cage pole, and (*iii*) the twelve "peripheral" μ_3-O(P), each bridging one six- and two five-coordinate tin atoms. The additional proton on the μ_2-OH is in the σ plane, to which its oxygen belongs, and oriented away from the C_3 axis. It gives the following distances and angles: H···Sn(CN = 6) = 2.54 Å; H···C = 3.37 Å (methyl of the six-coordinate tin atom); H···H = 1.65 Å (the hydrogen of the μ_2-OH); H–O–H = 110°; H–O–Sn(CN = 6) = 104°. The additional proton on the μ_3-O(I) is on the C_3 axis pointing towards the inside of the cluster. It gives the following distances and angle: H···Sn(CN = 6) = 2.68 Å; H···Sn (CN = 5) = 3.36 Å; H···μ_3-O(P) = 2.86 Å; H–O–Sn (CN = 6) = 116°. The additional proton on the μ_3-O(P) is on the outside of the Sn–O–Sn framework and aligned on the direction defined by the center of the cage and the μ_3-O(P) of interest. It gives the following distances and angles: H···Sn(CN = 6) = 2.53 Å; H···Sn(CN = 5) = 2.52 and 2.58 Å; H···C = 2.90 Å (methyl of the six-coordinate tin atom); H···C = 3.23 and 3.30 Å (methyl of the five-coordinate tin atom); H···H = 2.42 Å (methyl of the six-coordinate tin atom); H···H = 2.82 and 3.11 Å (methyl of the five-coordinate tin atom); H–O–Sn(CN = 6) = 101°; H–O–Sn (CN = 5) = 107 and 108°.

All the calculations were performed using the Gaussian 98 program,[61] on a Compaq Digital DS20 work station.

Results and discussion

Charge distributions

The charge distribution in the $[(MeSn)_{12}O_{14}(OH)_6]^{2+}$ macrocation is such that the hexacoordinated tin atoms have a more positive character than the pentacoordinated atoms. This can be concluded from the values of the net atomic charges (Table 1) based on the Mulliken and CHELPG populations analyses.[31,52] This feature means that the hexacoordinated tin atoms are slightly more suitable for interactions with negative species, electron donors or negative areas in the interacting molecule (nucleophilic attack), even though the two types of tin atoms have globally rather similar characteristics from the point of view of electrostatic interactions.

Table 1 Charges q [atomic units, Mulliken (M) and CHELPG (C)], softnesses S (eV^{-1}), hardnesses η (eV), condensed Fukui functions f^+ (atomic units) and condensed softnesses s_A^+ (calculated as $S \times f_A^+$) on the hexacoordinated (Sn_h) and pentacoordinated (Sn_p) tin atoms using HF and DFT (B3LYP)

Descriptor	B3LYP	HF
$q(Sn_h)$(M)	1.874	2.313
$q(Sn_p)$(M)	1.823	2.281
$q(Sn_h)$(C)	1.436	1.921
$q(Sn_p)$(C)	1.402	1.907
S	0.248	0.159
η	4.04	6.28
$f^+(Sn_h)$	0.023	0.0118
$f^+(Sn_p)$	0.030	0.0738
$s^+(Sn_h)$	0.00570	0.00094
$s^+(Sn_p)$	0.00740	0.00588

In view of these larger positive charges, the hexacoordinated tin atoms are expected to be harder, the pentacoordinated ones softer. Explicit calculations of the condensed local softness, given below, assess this proposal. Moreover, it should be realized that atomic charges as tabulated are isotropic as opposed to the acido-basic character of certain regions. MEP studies (*vide infra*) should therefore be used to confirm the indications of this "hard" indicator.

Fukui function and local softness

The condensed Fukui function f_A^+ [see eqn. (3)] was calculated for the two kinds of tin coordination present in $[(MeSn)_{12}O_{14}(OH)_6]^{2+}$ (Table 1). The higher the value of the Fukui function, the higher the probability for a nucleophilic attack involving a soft base to take place at that atom.

The local softness $s(\underline{r})$ is known to be a better indicator for intermolecular reactivity sequences than the Fukui function.[30a,39] This reactivity index was calculated for the two kinds of tin atoms present in $[(MeSn)_{12}O_{14}(OH)_6]^{2+}$, using eqn. (4). The HF results, which can be expected to be less reliable (*cf.* change of number of electrons pairs), are here given for the sake of completeness. Note, however, that the same ordering is obtained at both levels. The condensed form of the local softness (Table 1) indicates that the pentacoordinated tin atoms are the softest and, therefore, the hexacoordinated tin atoms are the hardest. This result is in agreement with the experimental observation (single crystal X-ray diffraction and/or ^{119}Sn NMR) that anions (Cl^-, $CH_3C_6H_4SO_3^-$, OH^-, $Ph_2PO_2^-$ and $CH_3CO_2^-$) interact with $[(^nBuSn)_{12}O_{14}(OH)_6]^{2+}$ at the cage poles, which are formed by the six-coordinate tin atoms.[5–7,9,10,14] Experimental data henceforth match computational predictions from the HSAB theory.[36–40] The next section examines whether this tendency is reflected in the MEP results and how the regioselectivity of neutral nucleophiles fits in this picture.

Molecular electrostatic potential (MEP)

MEP calculations were performed for two selected planes in order to assess whether the trend revealed by the softness calculations are confirmed, and also to compare the reactivity of the hexacoordinated and pentacoordinated tin atoms of $[(MeSn)_{12}O_{14}(OH)_6]^{2+}$.

In each plane, P1 and P2 (see Figs. 2 to 4), MEP contours show different spatial features for the penta- and hexacoordinated tin atoms. The two kinds of tin atoms are surrounded by positive potential regions, as expected from their charges (Table 1) and are, henceforth, appropriate for nucleophilic attack. However, the positive charges extend further away from the cage poles, the area in which the hexacoordinated

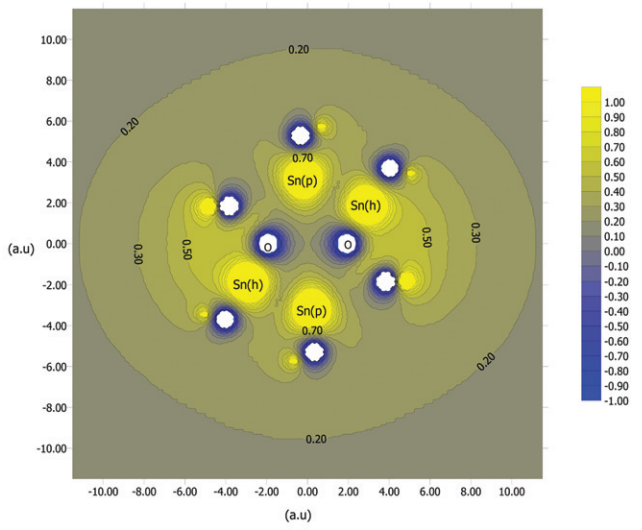

Fig. 3 MEP contour plot in the plane P1 shown in Fig. 2(a) (values in a.u.).

tin atoms are found, than from the cage equator, the area where the pentacoordinated tin atoms are located (see the 0.5 contour level in the Fig. 3 and 4). This difference between penta-and hexacoordinated tin turns out to be more pronounced at the B3LYP level than in the HF calculations (not shown). The distribution of the electrostatic potential (see Figs 3 and 4) around the five- and six-coordinated tin atoms explains the preference of nucleophiles for the polar part of the molecule or, more particularly, for the microcage formed by the (Sn-μ-OH)$_3$ moieties closed by the μ$_3$-O(I) atom. The high concentration of positive charge in the pole region means that this region has a higher acidic character than the equatorial part of the molecule, this being due to the cooperative influence of six electrophilic atoms (three Sn atoms and three protons). The influence of the electrophilic atoms is only partly counterbalanced by the four oxygens, since all the lone pairs are predominantly oriented outside the (Sn-μ-OH)$_3$ microcage. This is another application of a more general trend, already documented for polyoxometalates,[33] according to which the inner part of a convex cage is acidic, whereas the external part is basic. Hence, the nucleophile will approach preferentially the macrocation around the poles, that is the (Sn-μ-OH)$_3$

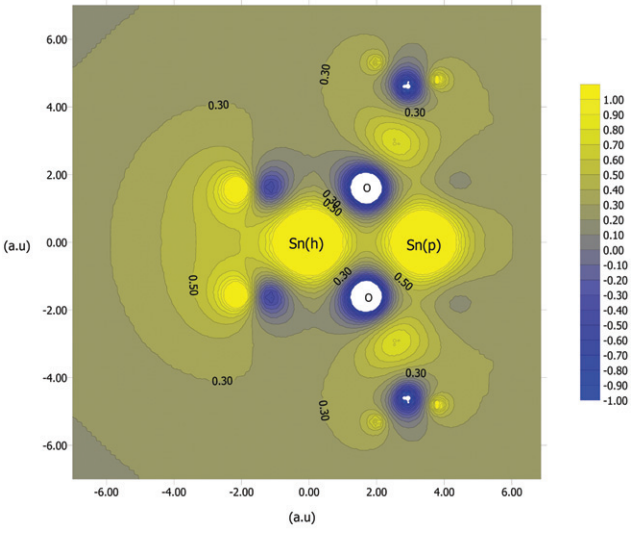

Fig. 4 MEP contour plot in the plane P2 shown in Fig. 2(b) (values in a.u.).

microcage, rather than the equator. This result is in agreement with the observations made on their charges and local softnesses when comparing the pentacoordinated and hexacoordinated tin atoms (see above). Even through the charge pattern of the Sn atoms is not opposite to the observed and calculated trend, care should be taken when comparing the small differences in calculated charges (Table 1) with the large gaps in stabilization energies reported in Table 2 (see below).

Stabilization energy

In order to assess the results above, a series of calculations was performed on the complexes resulting from the interaction between $[(MeSn)_{12}O_{14}(OH)_6]^{2+}$ and nucleophilic species of different hardness and softness: F^-, OH^-, Cl^-, H_2O, acetone and DMSO. The hardness sequence of the above nucleophiles is: H_2O (9.5 eV)[62] > F^- (7.0 eV)[62] > OH^- (5.7 eV)[62] > acetone (4.8 eV)[62,63] > Cl^- (4.7 eV)[62] > DMSO (3.6 eV).[64] The stabilization energies have been calculated for each of these nucleophiles interacting with the macrocation in the influence spheres of either the macrocation poles (hexacoordinated tin) or the macrocation equator (pentacoordinated tin). (See the Theory and Computational sections for geometry optimization details)

For the interaction with the cage pole, the following starting geometry was chosen: the nucleophiles were located on the C_3 axis at a X–μ$_2$-OH distance of 3.85 Å, which is much longer than the one encountered in a hydrogen bond (X is the nucleophile or its oxygen atom). For the nonatomic nucleophiles additional conditions were set. For OH^-, the O–H bond was on the C_3 axis with the H pointing away from the cage. For H_2O, the H–O–H bisector was on the C_3 axis, the H were pointing away from the cage and the H–O–H plane was perpendicular to a σ plane. For acetone, the C=O bond was on the C_3 axis, the methyl groups were pointing away from the cage and the plane defined by the three carbon atoms was perpendicular to a σ plane. For DMSO,[65] the S=O bond was on the C_3 axis, the plane defined by the oxygen, the sulfur and the bisector of the C–S–C angle was aligned with a σ plane and the methyl groups were oriented away from the cage and from the μ$_2$-OH toward which the DMSO was allowed to move (*vide infra*). From this starting geometry, two different optimizations were performed (see also Fig. 1). The nucleophile was allowed to move along the line defined by an oxygen of a μ$_2$-OH moiety and X [path A, *i.e.*, away from the C_3 axis, *d*(X–μ$_2$-OH] being the optimized variable), or along a line defined by a μ$_3$-O(I) and X {path B, *i.e.*, along the C_3 axis, *d*[X–μ$_3$-O(I)] being the optimized variable}. For nonatomic nucleophiles, the μ$_2$-OH moiety involved in route A is the one belonging to the σ plane used to defined the orientation of the nucleophile (*vide supra*). Path A appears as the most realistic one since the charge compensating anions, such as Cl^- or OH^-,[3,5,6,10] always form hydrogen bonds with a single particular μ$_2$-OH moiety, the other ones interacting with small neutral molecules containing oxygen (H_2O, *i*-PrOH, DMF, DMPU). By contrast, path B, which is more symmetrical, could account for an averaged solution behavior.

For the interactions with the pentacoordinated tin atoms in the area of the cage equator, the nucleophile was initially located on a C_2 axis with the distance X–Sn$_p$ set to 3.05 Å. Again, for the nonatomic nucleophiles, additional conditions need to be defined. For OH^-, the O–H bond was on the C_2 axis with the H oriented away from the cage. For H_2O, the H–O–H bisector was on the C_2 axis. For acetone and DMSO, the C=O or S=O bond was on the C_2 axis. For these three last cases, the hydrogen atoms or methyl groups were pointing away from the cage and the nucleophiles were oriented on the C_2 axis so as to maximize the shorter H···H contacts between the hydrogen atoms of the nucleophiles and the methyl groups of the pentacoordinated tin atoms. The optimization was performed along a line defined by X (the

Table 2 Stabilization energies resulting from the interaction between $[(MeSn)_{12}O_{14}(OH)_6]^{2+}$ and various nucleophiles at the cage equator (region of the 5-coordinate tin atoms) or at the cage poles (region of the 6-coordinate tin atoms),[a] as obtained at the B3LYP and Hartree–Fock levels.

	B3LYP		Hartree–Fock		
System	Energy/a.u.	Stabilization energy/kcal mol^{-1}	Energy/a.u.	Stabilization energy/kcal mol^{-1}	Stabilization energy BSSE/kcal mol^{-1}
$[(MeSn)_{12}O_{14}(OH)_6]^{2+}$	−2028.3392		−2015.9698		
OH^-	−75.7196		−75.3508		
OH^- at the cage pole (path A)[b]	−2104.3939	−210.21	−2091.6371	−198.6	−188.8
OH^- at the cage pole (path B)	−2104.3874	−206.14	−2091.6409	−201.0	−190.5
OH^- at the cage equator	−2104.2902	−145.15	−2091.5194	−124.7	−112.1
F^-	−99.7540		−99.4139		
F^- at the cage pole (path A)[b]	−2128.4340	−213.81	−2115.6806	−186.2	−175.4
F^- at the cage pole (path B)	−2128.4287	−210.47	−2115.6891	−191.7	−179.1
F^- at the cage equator	−2128.3549	−164.16	−2115.5866	−127.3	−113.7
Cl^-	−460.2522		−14.7504		
Cl^- at the cage pole (path A)[b]	−2488.8413	−156.80	−2030.9800	−163.0	−154.0
Cl^- at the cage pole (path B)	−2488.8385	−155.02	−2030.9835	−162.3	−155.8
Cl^- at the cage equator	−2488.7407	−93.63	−2030.8630	−89.6	−78.4
$(CH_3)_2SO$ (DMSO)	−553.1840		−163.7924		
$(CH_3)_2SO$ at the cage pole (path A)[b]	−2581.5680	−28.10	−2179.8312	−43.3	−40.3
$(CH_3)_2SO$ at the cage pole (path B)	−2581.5679	−28.06	−2179.8304	−42.7	−40.2
$(CH_3)_2SO$ at the cage equator	−2581.5332	−6.27	−2179.7816	−12.1	−11.1
$(CH_3)_2CO$ (acetone)	−193.1202		−191.8633		
$(CH_3)_2CO$ at the cage pole (path A)[b]	−2221.4986	−24.59	−2207.8828	−31.2	−29.5
$(CH_3)_2CO$ at the cage pole (path B)	−2221.4957	−22.76	−2207.8837	−31.7	−30.0
$(CH_3)_2CO$ at the cage equator	−2221.4664	−4.39	−2207.8454	−7.7	−6.7
H_2O	−76.3824		−75.9741		
H_2O at the cage pole (path A)[b]	−2104.7492	−17.31	−2091.9787	−21.8	−20.6
H_2O at the cage pole (path B)	−2104.7511	−18.54	−2091.9773	−21.0	−19.9
H_2O at the cage equator	−2104.7301	−5.35	−2091.9528	−5.6	−3.0

[a] See text for optimization geometries. [b] Path A: away from the C_3 axis; path B: along the C_3 axis.

nucleophile or its oxygen atom) and one of the neighboring pentacoordinated tin atoms, $d(X–Sn_p)$ being the only optimized variable.

The results of these "supermolecule" calculations at the B3LYP and HF levels for the fluoride, hydroxide and chloride anions, as well as for the water, acetone and DMSO molecules, are shown in Table 2.

First, one can note that, for all the nucleophiles, charged or uncharged, investigated, the stabilization energies are always larger (*i.e.*, more negative) in the neighborhood of the cage pole, as compared to the cage equator, meaning that they will interact preferentially with the poles. However, the stabilization energies involving the charged nucleophiles are unambiguously the largest (5 to 10 times larger than for the uncharged nucleophiles). These observations hold for the B3LYP as well as for the HF level, with or without BSSE corrections. It is seen that differences between two nucleophiles interacting with the cage pole and equator are very similar in both methods. The DFT differences OH^- (pole; path A) and OH^- (equator) $\approx$ 65.1 kcal mol^{-1} and F^- (pole; path A) and F^- (equator) $\approx$ 49.6 kcal mol^{-1} yield a difference value of −15.4 kcal mol^{-1}, which is almost identical to the −15 kcal mol obtained with Hartree–Fock, and similar for most other combinations. At least for the charged nucleophiles, this regioselectivity can be traced back to the higher positive charge of the 6-coordinate tin atoms, located at the cage poles, and is in line with the MEP results (Fig. 3 and 4). This result matches experimental NMR data in which the nature of the charge compensating anions hardly affects the ^{119}Sn chemical shift of the pentacoordinated tin atoms but modifies the one of the hexacoordinated ones.[5–7,9,10,14] For all nucleophiles and for both levels of calculation, no clear preference appears between paths A (away from the C_3 axis) and B (along the C_3 axis), as both optimization schemes yields very similar stabilization energies, whose differences are much smaller than the difference pole-equator. Both levels reveal the same nucleophilic ranking for the stabilization energies at the cage pole, except an inversion of OH^- and F^-, which in view of the high degree of filling of the valence orbitals in F^- and the numerically small differences, should not be overstated and should be looked upon with caution. In this view, differences obtained from the two methods in the absolute values of the interaction energies should not be overstated. The observed hardness order for the charged species is ($F^- > OH^- > Cl^-$) and matches perfectly the interaction energy sequence. In contrast, for the neutral nucleophiles the hardness order (H_2O > acetone > DMSO)[62–64] is reversed. Therefore, the interactions appear mainly associated with an electrostatic character and the formation of hydrogen bonds (*vide infra*). Accordingly, the MEP accounts succesfully for these interactions. This suggests that orbital controlled interactions between Lewis donors and acceptors are not decisive in the interactions between the nucleophiles and the cluster.

When OH^- and Cl^- are compared, the stabilization energies obtained do not appear to account for the experimentally observed easy exchange of the charge compensating hydroxide by chloride anions upon reacting $[(^nBuSn)_{12}O_{14}(OH)_6](OH)_2$ with 2 equivalents of HCl.[20] This discrepancy might be related to the part of the reaction that is not considered in the present calculation, the dissociation of HCl and the formation of H_2O, as the reaction was performed in poorly dissociating solvents (*e.g.*, THF).

The analysis of the optimized geometries (see Table 3) leads to some general comments. The difference between the two levels for the distances, at equilibrium, is remarkably small. Interestingly, and for both levels, all the nucleophiles appear attracted by the cage poles when considering the displacements from the starting positions. The closest approaches are observed for OH^- and F^-, then for DMSO and finally for Cl^-, acetone and water. Moreover, even if no clear energetic

Table 3 Selected interatomic distances for the optimized geometries of the interactions between $[(MeSn)_{12}O_{14}(OH)_6]^{2+}$ and various nucleophiles at the cage poles (region of the 6-coordinate tins),[a] as obtained at the B3LYP and HF levels

		B3LYP		HF	
Nucleophile	Distance[b]	Path A[c]	Path B[c]	Path A[c]	Path B[c]
OH^-	d(X–μ_2-OH)	**2.36**/3.08	2.65	**2.38**/3.09	2.69
	d(X–Sn_h)	3.45/3.99	3.43	3.47/4.00	3.48
	d(X–μ_3-O)	4.00	**3.78**	4.02	**3.83**
F^-	d(X–μ_2-OH)	**2.32**/3.00	2.59	**2.38**/3.09	2.61
	d(X–Sn_h)	3.42/3.98	3.37	3.47/4.00	3.38
	d(X–μ_3-O)	3.97	**3.69**	4.02	**3.71**
Cl^-	d(X–μ_2-OH)	**2.95**/3.22	3.09	**2.97**/3.34	3.10
	d(X–Sn_h)	3.94/4.24	3.93	3.96/4.25	3.94
	d(X–μ_3-O)	4.48	**4.36**	4.50	**4.37**
DMSO	d(X–μ_2-OH)	**2.76**/3.11	3.03	**2.70**/3.21	3.02
	d(X–Sn_h)	3.79/4.16	3.85	3.74/4.13	3.84
	d(X–μ_3-O)	4.33	**4.27**	4.28	**4.25**
Acetone	d(X–μ_2-OH)	**2.85**/3.28	3.03	**2.86**/3.29	3.07
	d(X–Sn_h)	3.86/4.19	3.86	3.87/4.20	3.91
	d(X–μ_3-O)	4.40	**4.28**	4.41	**4.33**
H_2O	d(X–μ_2-OH)	**2.87**/3.28	3.18	**2.97**/3.34	3.27
	d(X–Sn_h)	3.87/4.20	4.03	3.96/4.25	4.12
	d(X–μ_3-O)	4.40	**4.47**	4.49	**4.57**

[a] See text for optimization geometries. [b] X corresponds to the nucleophile or to its oxygen atom. [c] Path A: away from the C_3 axis; path B: along the C_3 axis. For path A, the displacement of the nucleophile away from the C_3 axis leads to two d(X–μ_2-OH) and d(X–Sn_h) distances, in a 1 : 2 and 2 : 1 ratio, respectively. The bold figures correspond to the optimized variables.

preferences could be found between paths A and B, the latter always leads to a nucleophile closer to the pole as shown by smaller d(X–μ_3-O) values. Most of the X–μ_2-OH distances (the shorter in path A) agree with the formation of hydrogen bonds.[66] For OH^- and Cl^-, these distances compare reasonably well with the minimum d(X–μ_2-*O*H) found in the crystal structure of $[(^nBuSn)_{12}O_{14}(OH)_6](OH)_2(HO^iP_r)_4$ and $[(^nBuSn)_{12}O_{14}(OH)_6]Cl_2(H_2O)_2$, which are 2.68 and 3.04 Å, respectively.[5,6] With, maybe, the exception of OH^- and F^-, which interact most strongly with the cage pole, the X–Sn_h distances do not indicate any contacts between the nucleophiles and the hexacoordinated tin atoms. This last point stresses the absence of Lewis interactions between the nucleophiles and the cage pole tin atoms.

For H_2O, which is the hardest nucleophile considered,[62–64] the stabilization energies are anyhow the smallest. Its preferential interaction with the cage pole is in line with the presence of the harder tin atoms in this region. Nevertheless, the X–μ_2-OH distances indicate the likely formation of hydrogen bonds. This result matches the experimental observation of hydrogen bonds in all the structures that involve water molecules.[3,5] The larger stabilization energies observed at the cage poles, which drive the water molecules toward this region, could explain, at least in part, why the oxygen exchange experienced by the macrocation upon exposure to water, and which can be followed by ^{17}O NMR,[67] is much faster at μ_2-OH bridge positions than at the peripheral μ_3-O(P) oxygens.

With acetone and DMSO, two fairly soft nucleophiles,[62–64] the more stable "supermolecules" again correspond to an interaction at the cage poles and not at the softer equatorial region (Table 2). Hydrogen bonds are very likely involved (Table 3) in such a feature. Moreover, the stronger interaction, according to the stabilization energies, observed for DMSO at the cage pole, as compared to acetone, can be traced back to its greater facility to form hydrogen bonds. The Mulliken charges[31] for the oxygen of the DMSO, interacting at its optimized position with the macrocation, are −0.69 and −1.03 for the B3LYP level and for the HF level, respectively, while, for the oxygen of acetone, also in its optimized interaction geometry, they are −0.52 and −0.62, for the B3LYP level and for the HF level, respectively. These charges indicate a more polarized S=O bond, as compared to the C=O one, the former being therefore more prone to hydrogen bond formation. Indeed, the d(X–μ_2-OH) distance obtained for both basis sets (Table 3) is always shorter for DMSO than for acetone. Yet, ^{119}Sn NMR data obtained on $[(BuSn)_{12}O_{14}(OH)_6](Ph_2PO_2)_2$ show a 10 ppm shift to lower frequency and a broadening, for the ^{119}Sn resonance of the pentacoordinated tin only, upon substituting CD_2Cl_2 for acetone-d_6. Such a shift is, undoubtedly, the evidence for an interaction in solution between the Lewis base and the pentacoordinated tin atoms, as shown in the solid state for $[(BuSn)_{12}O_{14}(OH)_6](4\text{-}CH_3C_6H_4SO_3)_2{\cdot}C_4H_8O_2$.[10] However, this interaction is very weak since the effects on the resonance of the pentacoordinated tin atoms are observable with a 4000-fold excess of acetone, but not with a 25-fold excess. The $[(BuSn)_{12}O_{14}(OH)_6](4\text{-}CH_3C_6H_4SO_3)_2$ compound in acetone does not even show any ^{119}Sn resonance shift at all (when compared to CD_2Cl_2), evidencing that, in addition to being very weak, the interaction of acetone with the cluster is modulated by the nature of the counteranion, a factor that could not be considered in our calculations. Such a critical influence of the charge compensating anions was also observed for DMSO. Thus, when the anions are *p*-toluene sulfonates, the rupture of the anion-macrocation electrostatic interaction was experimentally established.[10] This makes the cage poles accessible and DMSO molecules can interact with the μ_2-OH bridges, as seen from $^2J(^1H\text{-}O\text{-}^{119}Sn_{hexa})$ coupling data and a slight influence of DMSO on the ^{119}Sn chemical shift of the 6-coordinate tin atoms.[10] However, when the counteranions are diphenyl phosphinates, DMSO dissociates the macrocation-anion complex to a much lesser extent, which disfavors the access to the cage pole, at the profit of an interaction with the pentacoordinated tin atoms, again evidenced by their low ^{119}Sn frequency shift.[7] Other experimental evidence for interactions between Lewis bases and the five-coordinate tin atoms was also obtained by ^{119}Sn NMR for which a shielding of the resonance associated with the five-coordinate tin atoms is observed, in solution, when $[(BuSn)_{12}O_{14}(OH)_6]Cl_2$ is in the presence of THF or pyridine.[20] This type of interaction does not appear in the calculations presented here, likely because of the competition between such a weak interaction and the formation of hydrogen bonds. The polarization induced by the unbalanced charge of the macrocation might also be involved in the preferential interaction of the soft nucleophiles with the cage poles. The competitive and simultaneous presence of a charge compensating anion (actually two are needed to neutralize the macrocation) and of a soft Lewis base was not possible to calculate within a reasonable time.

Even though they do not correspond to the stronger interactions, and keeping in mind the limitation, discussed above, on the simultaneous presence of an anion and Lewis base, some comments can be made on the optimized geometries at the equator, in the vicinity of the 5-coordinate tin atoms. For OH^- and F^-, the optimized X–Sn_p distances decrease, when compared to the starting geometry (3.05 Å) In the HF level these distances are 2.83 and 2.96 Å, for OH^- and F^-, respectively. For the B3LYP level there is an inversion in these distances and the F^- (2.54 Å) is now closer than the OH^- (3.03 Å), in accordance with the interaction energy sequence. The other nucleophiles are pushed away from the pentacoordinated tin, though to different extents. The final distances are, in B3LYP, 3.46, 5.13, 5.16 and 5.48 Å and, in HF, 3.53, 5.27, 5.53, 5.57 Å, for Cl^-, DMSO, acetone and water, respectively.

Last but not least, in spite of both the very demanding and time consuming calculations, and, as a result of this, the rather restrictive spatial constraints as to how the nucleophiles can approach their site of interactions, the results obtained for the stabilization energies between both regions of the cluster and the nucleophiles match satisfactorily the experimental data in hand and, in general, show a self-consistency when the results from the B3LYP and HF methods are compared.

Basicity of the cluster oxygen atoms

As described above (Computational details) the macrocation contains three types of oxygens: six μ_2-OH oxygens, two "internal" μ_3-O(I) oxygens, and twelve "peripheral" μ_3-O(P) oxygens. The charges found for these oxygens are shown in Table 4. The agreement between the two population analysis methods (Mulliken[31] and CHELPG[52] populations) is not satisfactory since the Mulliken populations obey the sequence μ_3-O(I) > μ_3-O(P) > μ_2-OH (in absolute values) whereas the CHELPG populations obey the sequence μ_3-O(P) > μ_2-OH > μ_3-O(I). The origin of this discrepancy may be related to the internal, and therefore shielded, position of the oxygen μ_3-O(I) as CHELPG charges are calculated by fitting the actual potential to the one arising from these charges. *A priori* the basicity of the oxygen atoms can be assessed either by charge calculations or by the stabilization energy for protonation.

The stabilization energy upon protonation was calculated as the difference between the energy of the macrocation protonated at the oxygen of interest (O–H^+) and the energy of the macrocation alone. For each oxygen, the H^+ was placed at a distance of 1.0 Å, according to the geometries detailed in the 'Theory and Computational details' sections, which correspond to tetrahedral configurations for the protonated oxygens. In particular, for the μ_3-O(I) oxygen, this means that the proton is located inside the cage. The results are shown in Table 5. Whatever the method used, the basicity sequence is found as μ_3-O(P) > μ_3-O(I) > μ_2-OH. Note that the sequence of charges is not appropriate as a basicity indicator in this present case, because it does not take into account the accessibility effect of the oxygen to the protons, which is extremely different for the three oxygens. The molecular topology and the MEP (Figs. 1, 3 and 4) clearly indicated that the incoming proton cannot access the most basic side of the μ_3-O(I) oxygen, which is opposite to the tripod of hexacoordinated Sn atoms. At variance with this situation, the μ_3-O(P), opposite to the metal tripod, is clearly accessible to the proton and this explains its greater protonation energy (see Table 5). Therefore, we considered the stabilization energies as the only appropriate basicity indicator in this study

Considering that ^{17}O NMR data (*vide supra*) have revealed, in the presence of water, a much faster exchange of the μ_2-OH than of the μ_3-O oxygens, it can be concluded that the basicity of the oxygens, as reflected by the results of Table 5, is not the main factor determining the exchange rate. This suggests further that the preferred interaction of water with the cage poles (*vide supra*) could facilitate the nucleophilic attack of a hexacoordinated tin by H_2O. This entering water molecule, ^{17}O enriched to follow the reaction, forms a Sn–$^{17}OH_2$ bond and turns a μ_2-OH into a terminal OH moiety to maintain the hexacoordination at tin. Ultimately, after a proton transfer from the bonded water to the terminal OH, an unenriched water molecule is released into the medium, as experimentally observed.

Table 4 Charges on the oxygen atoms and on the μ_2-OH hydrogens of $[(MeSn)_{12}O_{14}(OH)_6]^{2+}$, calculated at the B3LYP and HF levels[a]

	B3LYP		HF	
Oxygen	Mulliken	CHELPG	Mulliken	CHELPG
μ_2-O<u>H</u>	−0.936	−0.764	−1.103	−1.035
μ_3-O(P)	−1.059	−0.840	−1.335	−1.170
μ_3-O(I)	−1.072	−0.604	−1.340	−0.672
μ_2-O<u>H</u>	+0.460	+0.297	+0.483	+0.473

[a] Oxygen labelling: P = peripheral; I = internal.

Table 5 Energies of the $\{[(MeSn)_{12}O_{14}(OH)_6]^{2+} + H^+\}$ complexes, as well as protonation energies ($E_{cage+H} - E_{cage}$), calculated at the B3LYP and HF levels

Protonation site/method	μ_2-OH	μ_3-O(P)	μ_3-O(I)
Energy[a] /a.u.			
B3LYP	−2028.4372	−2028.4822	−2028.4789
HF	−2016.0536	−2016.0966	−2016.0758
Protonation energy/kcal mol^{-1}			
B3LYP	−61.5	−89.7	−87.6
HF	−52.5	−79.6	−66.4

[a] The energies for the unprotonated cage are −2028.3392 and −2015.9698 a.u., with the B3LYP and HF methods, respectively, see Table 2.

Conclusions

As a whole, the hardness/softness properties of tin atoms are obviously modulated by their coordination, and hence influence the type of interactions they can undergo. Yet, the sole consideration of the hardness/softness at the local level, associated with the HSAB principle, is not sufficient to predict in all the cases the strength and orientation of the interaction between various nucleophiles and the macrocation $[(RSn)_{12}O_{14}(OH)_6]^{2+}$. Electrostatic interactions at a global level and hydrogen bonds, taking place locally at the cage poles, have to be considered and apparently constitute the predominant effect. Accordingly, the molecular electrostatic potential and the atomic charges, in the case of harder atoms, adequately represent the interaction geometry, especially with anionic species.

The two methods method used in the present work (B3LYP and HF) lead to the same qualitatively and quantitatively similar description of the chemistry and reactivity of the monocluster $[(RSn)_{12}O_{14}(OH)_6]^{2+}$ and yield reasonable agreement with the relevant experiment results.

The main output of these theoretical calculations is that, unlike many organotin compounds that are prone to coordination extension through orbital controlled interactions between Lewis donors and the tin atom acting as the Lewis acid, the interactions between the $[(RSn)_{12}O_{14}(OH)_6]^{2+}$ cluster and nucleophiles are mostly dictated by electrostatic forces and hydrogens bonds at the cages poles. Orbital controlled interactions play only a minor role at the level of the five-coordinated tin atoms at the equator of the cage.

These results illustrate that present-day quantum chemical computational techniques, accompanied by recently developed DFT concepts and supported by dramatic computer hardware progress, have now reached a sufficient degree of maturity to be really useful tools in the understanding of systems whose size was a problem and were thus unthinkable to address up to very recently. The interplay between experiment and theory at the molecular level largely benefits from this evolution.

Acknowledgements

P. G. is indebted to the Fund for Scientific Research Flanders (Belgium)(FWO), and the Research Council of the Free

University of Brussels (VUB), for continuous support to the group. R. V.-R. thanks the Colombian Institute for Science and Development, ColCiencias, and the Universidad de Cartagena (Cartagena, Colombia) for a PhD fellowship. M. B. and R. W. are indebted to the Fund for Scientific Research Flanders (Belgium, grant nr G0192.98) for financial support. F. R., C. S., M. B. and R. W. are indebted to the Flemish Ministry of Education and the French Ministries of Foreign Affairs and Education, Research and Technology for the allocation of a Tournesol Grant (nr 99.091). The authors wish to thank Prof. O. Eisenstein for numerous constructive remarks on an early version of this text, and an anonymous referee for his suggestions for further improvement.

References

1 R. R. Holmes, *Acc. Chem. Res.*, 1989, **22**, 190.
2 H. Puff and H. Reuter, *J. Organomet. Chem.*, 1989, **368**, 173.
3 H. Puff and H. Reuter, *J. Organomet. Chem.*, 1989, **373**, 173.
4 H. Reuter, *Angew. Chem.*, 1991, **103**, 1487.
5 D. Dakternieks, H. Zhu, E. R. T. Tiekink and R. Colton, *J. Organomet. Chem.*, 1994, **476**, 33.
6 F. Banse, F. Ribot, P. Toledano, J. Maquet and C. Sanchez, *Inorg. Chem.*, 1995, **34**, 6371.
7 F. Ribot, C. Sanchez, R. Willem, J. C. Martins and M. Biesemans, *Inorg. Chem.*, 1998, **37**, 911.
8 P. Jaumier, B. Jousseaume, M. Lahcini, F. Ribot and C. Sanchez, *Chem. Commun.*, 1998, 369.
9 C. Eychenne-Baron, F. Ribot and C. Sanchez, *J. Organomet. Chem.*, 1998, **567**, 137.
10 C. Eychenne-Baron, F. Ribot, N. Steunou, C. Sanchez, F. Fayon, M. Biesemans, J. C. Martins and R. Willem, *Organometallics*, 1940, **19**, 2000.
11 F. Ribot, F. Banse, C. Sanchez, M. Lahcini and B. Jousseaume, *J. Sol-Gel Sci. Technol.*, 1997, **8**, 529.
12 F. Ribot, C. Eychenne-Baron and C. Sanchez, *Phosphorus, Sulfur Silicon Relat. Elem.*, 1999, **41**, 150–151.
13 L. Angiolini, D. Caretti, R. De Vito, F. T. Niesel, E. Salatelli, C. Carlini, F. Ribot and C. Sanchez, *J. Inorg. Organomet. Polym.*, 1998, **7**, 151.
14 F. Ribot, F. Banse, F. Diter and C. Sanchez, *New J. Chem.*, 1995, **19**, 1145.
15 F. Ribot, C. Eychenne-Baron and C. Sanchez, *Mater. Res. Soc. Symp. Proc.*, 1998, **519**, 29.
16 F. Ribot and C. Sanchez, *Common. Inorg. Chem.*, 1999, **20**, 327.
17 (*a*) V. W. Day, T. A. Eberspacher, W. G. Klemperer and C. W. Park, *J. Am. Chem. Soc.*, 1993, **115**, 8469; (*b*) N. Steunou, F. Robert, K. Boubeker, F. Ribot and C. Sanchez, *Inorg. Chim. Acta*, 1998, **279**, 144.
18 A. Müller, R. Rohlfing, E. Krickemeyer and H. Bögge, *Angew. Chem. Int. Ed. Engl.*, 1993, **32**, 909.
19 G. Kastner and H. Reuter, *J. Organomet. Chem.*, 2000, **598**, 381.
20 F. Ribot, G. Kehr and C. Sanchez, unpublished results.
21 K. A. Nguyen, M. T. Carroll and M. S. Gordon, *J. Am. Chem. Soc.*, 1991, **113**, 7924.
22 A. Papakondylis, A. Mavridis and B. Bigot, *J. Phys. Chem.*, 1994, **98**, 8906.
23 A. Gobbi and G. Frenking, *J. Am. Chem. Soc.*, 1994, **116**, 9287.
24 A. Marquez, G. G. Gonzalez and F. Fernandez-Sanz, *Chem. Phys.*, 1989, **138**, 99.
25 J. Leszczynski and I. J. Yanov, *J. Phys. Chem. A.*, 1999, **103**, 396.
26 C. H. Schiesser, M. L. Styles and L. M. Wild, *J. Chem. Soc. Perkin Trans. 2*, 1996, 2257.
27 (*a*) M. A. Buntine, V. J. Hall, F. J. Kosovel and E. R. T. Tiekink, *J. Phys. Chem. A*, 1998, **102**, 2472; (*b*) M. A. Buntine, V. J. Hall, F. J. Kosovel and E. R. T. Tiekink, *Z. Kristallogr.*, 1998, **213**, 669; (*c*) E. R. T. Tiekink, V. J. Hall, J. Hook and M. A. Buntine, *Z. Kristallogr.*, 2000, **215**, 23; (*d*) E. R. T. Tiekink, V. J. Hall and M. A. Buntine, *Z. Kristallogr.*, 1999, **214**, 124.
28 (*a*) D. Duca, G. Barone, G. La Manna, T. Fiore, C. Pellerito, R. Di Stefano, M. Scopello and L. Pellerito, *Appl. Organometal. Chem.*, 2001, **15**, 581; (*b*) G. Barone, M. C. Ramusino, R. Barbieri and G. La Manna, *J. Mol. Struct. (Theochem).*, 1999, **469**, 143.
29 R. Vivas-Reyes, F. De Proft, M. Biesemans, R. Willem and P. Geerlings, *J. Phys. Chem. A.*, 2002, **106**, 2753.
30 (*a*) R. G. Parr and W. Yang, *Density Functional Theory of Atoms and Molecules*, Oxford University Press, New York, 1989; (*b*) R. G. Parr and W. Yang, *Annu. Rev. Phys. Chem.*, 1995, **46**, 701; (*c*) H. Chermette, *J. Comp. Chem.*, 1999, **20**, 129; (*d*) P. Geerlings, F. De Proft and W. Langenaeker, *Chem. Rev.*, submitted
31 R. S. Mulliken, *J. Chem. Phys.*, 1955, **23**, 1833.
32 R. Bonaccorsi, E. Scrocco and J. Tomasi, *J. Chem. Phys.*, 1970, **51**, 5270.
33 (*a*) J. Y. Kempf, M. M. Rohmer, J. M. Poblet, C. Bo and M. Bénard, *J. Am. Chem. Soc.*, 1992, **114**, 1136; (*b*) M. M. Rohmer, M. Bénard, J. P. Blaudeau, J. P. Maestre and J. M. Poblet, *Coord. Chem. Rev.*, 1998, **178–180**, 1019 and references cited therein; (*c*) E. Espinosa, C. Lecomte, N. E. Ghermani, J. Devemy, M. M. Rohmer, M. Bérnard and E. Molins, *J. Am. Chem. Soc.*, 1996, **118**, 2501.
34 (*a*) R. G. Parr and R. G. Pearson, *J. Am. Chem. Soc.*, 1983, **105**, 512; (*b*) R. G. Parr and W. Yang, *J. Am. Chem. Soc.*, 1984, **106**, 4049
35 W. Yang and R. G. Parr, *Proc. Natl. Acad. Sci. USA.*, 1985, **82**, 6723.
36 R. G. Pearson, *J. Am. Chem. Soc.*, 1963, **85**, 3533.
37 R. G. Pearson, *Coord. Chem. Rev.*, 1990, **100**, 403.
38 P. Geerlings, F. De Proft and W. Langenaeker, in *Density Functional Methods: Applications in Chemistry and Material Science*, ed. M. Springborg, John Wiley, New York, 1997.
39 P. Geerlings, F. De Proft and W. Langenaeker, *Adv. Quantum Chem.*, 1999, **33**, 303.
40 P. Geerlings and F. De Proft, *Int. J. Quant. Chem.*, 2000, **80**, 225.
41 J. L. Gazquez and F. Mendez, *J. Phys. Chem.*, 1994, **98**, 4591.
42 S. Damoun, G. Van de Woude, F. Mendez and P. Geerlings, *J. Phys. Chem. A.*, 1997, **101**, 866.
43 F. Mendez, F. Tamariz and P. Geerlings, *J. Phys. Chem. A*, 1998, **102**, 6292.
44 F. Mendez, M. L. de Romero, F. De Proft and P. Geerlings, *J. Org. Chem.*, 1998, **63**, 5774.
45 (*a*) T. N. Le, L. T. Nguyen, F. De Proft, A. K. Chandra, P. Geerlings and M. T. Nguyen, *J. Chem. Soc., Perkin Trans. 2*, 1999, 1249; (*b*) L. T. Nguyen, F. De Proft, M. T. Nguyen and P. Geerlings, *J. Chem. Soc., Perkin Trans. 2*, 2001, 818; (*c*) L. T. Nguyen, F. De Proft, M. T. Nguyen and P. Geerlings, *J. Org. Chem.*, 2001, **66**, 6096.
46 L. T. Nguyen, T. N. Le, F. De Proft, A. K. Chandra, W. Langenaeker, M. T. Nguyen and P. Geerlings, *J. Am. Chem. Soc.*, 1999, **121**, 5992.
47 C. Lee, W. Yang and R. G. Parr, *J. Mol. Struct.*, 1988, **163**, 305.
48 W. Yang and W. J. Mortier, *J. Am. Chem. Soc.*, 1986, **108**, 5708.
49 D. Mirejorsky, W. Drenth and F. B. Van Duijneveldt, *J. Org. Chem.*, 1978, **43**, 763.
50 M. Tielemans, R. Areschka, J. Colomer, R. Promel, W. Langenaeker and P. Geerlings, *Tetrahedron*, 1992, **48**, 10575.
51 W. Langenaeker, F. De Proft and P. Geerlings, *J. Phys. Chem. A*, 1998, **102**, 5994.
52 C. M. Breneman and K. B. Wiberg, *J. Comp. Chem.*, 1990, **11**, 361.
53 P. J. Hay and W. R. Wadt, *J. Chem. Phys.*, 1985, **82**, 270.
54 W. R. Wadt and P. J. Hay, *J. Chem. Phys.*, 1985, **82**, 284.
55 P. J. Hay and W. R. Wadt, *J. Chem. Phys.*, 1985, **82**, 299.
56 (*a*) A. D. Becke, *J. Chem. Phys.*, 1993, **98**, 5648; (*b*) C. Lee, W. Yang and R. G. Parr, *Phys. Rev. B*, 1998, **37**, 785; (*c*) P. J. Stephens, F. J. Delvin, C. F. Chablowski and M. J. Firsch, *J. Phys. Chem.*, 1994, **98**, 11623.
57 W. J. Hehre, L. Radom, L. P. v. R. Schleyer and J. A. Pople, *Ab Initio Molecular Orbital Theory*, Wiley, New York, 1986.
58 W. Koch and M. C. A. Holthausen, *Chemist's Guide to Density Functional Theory*, Wiley-VCH, Weinheim, 2000, p. 117.
59 F. B. Van Duijneveldt, J. G. C. M. Van Duijneveldt-Van De Rijdt and J. H. Van Lenthe, *Chem Rev.*, 1994, **94**, 1873.
60 J. O. Lundgren and J. M. Williams, *J. Chem. Phys.*, 1973, **58**, 788.
61 M. J. Frisch, G. W. Trucks, H. B. Schlegel, G. E. Scuseria, M. A. Robb, J. R. Cheeseman, V. G. Zakrzewski, J. A. Montgomery, R. E. Stratmann, J. C. Burant, S. Dapprich, J. M. Millam, A. D. Daniels, K. N. Kudin, M. C. Strain, O. Farkas, J. Tomasi, V. Barone, M. Cossi, R. Cammi, B. Mennucci, C. Pomelli, C. Adamo, S. Clifford, J. Ochterski, G. A. Petersson, P. Y. Ayala, Q. Cui, K. Morokuma, D. K. Malick, A. D. Rabuck, K. Raghavachari, J. B. Foresman, J. Cioslowski, J. V. Ortiz, B. B. Stefanov, G. Liu, A. Liashenko, P. Piskorz, I. Komaromi, R. Gomperts, R. L. Martin, D. J. Fox, T. Keith, M. A. Al-Laham, C. Y. Peng, A. Nanayakkara, C. Gonzalez, M. Challacombe, P. M. W. Gill, B. G. Johnson, W. Chen, M. W. Wong, J. L. Andres, M. Head-Gordon, E. S. Replogle and J. A. Pople, Gaussian 98 (Revision A.7), Gaussian, Inc., Pittsburgh, PA, 1998.
62 R. G. Pearson, *Inorg. Chem.*, 1988, **27**, 734.

63 C. Desfrancois, H. Abdoul-Carime, N. Khelifa and J. P. Shermann, *Phys. Rev. Lett.*, 1994, **73**, 2436.
64 K. Choho, K. G. Van Lier, G. Van de Woude and P. Geerlings, *J. Chem. Soc., Perkin Trans. 2*, 1996, 1723.
65 Because of the lone pair on the sulfur atom, the DMSO molecular structure is expected to be nonplanar (*i.e.*, different from acetone). Therefore, the internal geometry of a free DMSO molecule was fully optimized prior to the interaction computation, using the 6-31++G** basis set. The resulting distances and angles are : d(S–O) = 1.49 Å, d(S–C) = 1.80 Å, $\angle$ (O–S–C) = 106.3° and $\angle$ (C–S–C) = 98.2°. These angles clearly confirm the nonplanarity of DMSO.
66 (*a*) A. Novak, *Struct. Bonding (Berlin)*, 1974, **18**, 177; (*b*) F. Hibbert and J. Emsley, *Adv. Phys. Org. Chem.*, 1990, **26**, 255; (*c*) L. J. Bellamy and A. J. Owen, *Spectrochim. Acta, Part A*, 1969, **25**, 329; (*d*) W. Mikenda, *J. Mol. Struct.*, 1986, **147**, 1.
67 F. Ribot, C. Sanchez, C. Eychenne-Baron, R. Willem and M. Biesemans, unpublished results.